Microstructure and Microwave Dielectric Properties of $(1-x)Ba(Co_{1/3}Nb_{2/3})O_3-xBa(Zn_{1/3}Nb_{2/3})O_3$ Ceramics

Byung-Guk Ahn, Cheol-Woo Ahn,* Sahn Nahm,[†,*] and Hwack-Joo Lee**

Faculty of New Materials Engineering, Chonbuk National University, Chonju 561-756, Korea
*Department of Materials Science and Engineering, Korea University, Seoul 136-701, Korea
**New Materials Evaluation Center, Korea Research Institute of Standards and Science,
Taeduk Science Town, Taejon 305-600, Korea

ABSTRACT

$Ba(Co_{1/3}Nb_{2/3})O_3$(BCN) has a $1:2$ ordered hexagonal structure. Q-value of BCN increased with increasing sintering temperature however, it significantly decreased when the sintering temperature exceeded 1400°C. $Ba(Zn_{1/3}Nb_{2/3})O_3$(BZN) has the 1:2 ordered hexagonal structure and the degree of the $1:2$ ordering decreased with the increase of the sintering temperature. The Q-value of the BZN increased with increasing the sintering temperature and BZN sintered at 1400°C for 6 h has a maximum Q-value. For $(1-x)Ba(Co_{1/3}Nb_{2/3})O_3-xBa(Zn_{1/3}Nb_{2/3})O_3$ [(1-x)BCN-xBZN] ceramics, the $1:2$ ordered hexagonal structure was observed in the specimens with $x \leq 0.3$ and the $BaNb_6O_{16}$ second phase was found in the specimens with $x \geq 0.6$. Grain growth, which is related to the $BaNb_6O_{16}$ second phase occurred in the specimens with $x \geq 0.5$. In this work, the excellent microwave dielectric properties of τ_f=0.0 ppm/°C, ε_r=34.5 and Q×f=97,000 GHz were obtained for the 0.7BCN-0.3BZN ceramics sintered at 1400°C for 20 h.

Key words : Microstructure, Microwave dielectric properties, Niobates

1. Introduction

R ecently, investigations on the Nb_2O_5 based complex perovskite ceramics has been increased to replace the expensive Ta-based complex perovskite ceramics for the application of microwave devices.[1-3] However, since the complicated microstructures such as liquid phase and grain growth usually develop in the Nb_2O_5-based complex ceramics, the understanding of both the structural variation and its effects on the microwave dielectric properties is necessary to obtain the required microwave dielectric properties. In the case of $Ba(Zn_{1/3}Nb_{2/3})O_3$ (BZN) and $Ba(Ni_{1/3}Nb_{2/3})O_3$ (BNN) ceramics, many investigations carried out on the structural variation and its effect on the microwave dielectric properties.[2-4] However, the microstructure of the BCN ceramic has not been clearly understood.

According to the previous works, BZN and BNN ceramics have the negative τ_f and BCN has the positive τ_f therefore, the (1-x)BCN-xBNN and (1-x)BCN-xBZN solid solutions have been studied to obtain a new material which has zero τ_f.[5,6] Especially, BZN has a high dielectric constant and a high Q-value, the (1-x)BCN-xBZN solid solution was expected to have excellent microwave dielectric properties.[5,7] However, even though many investigations have

been conducted on the (1-x)BCN-xBZN ceramics, the microstructure and microwave dielectric properties of the (1-x) BCN-xBZN ceramics have not been completely understood.[8] In this work, BCN, BZN and (1-x)BCN-xBZN ceramics were produced under various process conditions and the microstructure and the microwave dielectric properties were studied. Especially, the variation of Q-value was explained in terms of the structural changes.

2. Experimental Procedures

Ceramics of the composition $(1-x)Ba(Co_{1/3}Nb_{2/3})O_3-xBa(Zn_{1/3}Nb_{2/3})O_3$ with $0.0 \leq x \leq 1.0$ were prepared from the oxides of > 99% purity by using conventional solid state synthesis. Oxide compounds of $BaCO_3$, CoO, ZnO, and Nb_2O_5 were mixed for 18~24 h in a nylon jar with zirconia balls and then dried and calcined at 1100~1200°C for 3~4 h. After remilling, the powder was dried and pressed into discs and sintered at 1300~1550°C. The sintered specimens were cooled inside the furnace. The cooling rate was about 20°C/min until the temperature decreased to 800°C, but it was difficult to measure the cooling rate below 800°C. The microstructure of the specimen was studied by X-Ray Diffraction (XRD : Rigaku D/max-RC), Scanning Electron Microscopy (SEM : Hitachi S-4300) and High Resolution Transmission Electron Microscope(HRTEM: Hitachi H-9000-NAR TEM). The densities of the sintered specimens were measured by water-immersion technique. The dielectric properties were measured around 8.5−9.0 GHz at room temperature by a

---
[†]Corresponding author : Sahn Nahm

E-mail : snahm@korea.ac.kr

Tel : +82-2-3290-3279   Fax : +82-2-928-3584

dielectric post resonator technique suggested by Hakki-Coleman[9] and Courtney.[10] The temperature coefficient of the resonant frequencies were measured at 6.5 GHz in the temperature range of 25 and 85°C.

3. Results and Discussion

3.1. Microstructure and Microwave Dielectric Properties of Ba(Co₁/₃Nb₂/₃)O₃ Ceramics

Fig. 1 shows X-ray diffraction patterns of BCN ceramics sintered at various temperatures for 6 h. All the peaks were indexed in terms of the 1 : 2 ordered hexagonal unit cell. The
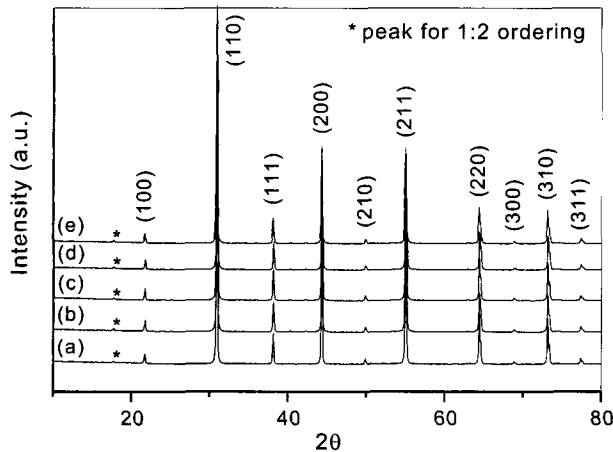

Fig. 1. XRD patterns of BCN ceramics sintered at: (a) 1350°C, (b) 1400°C, (c) 1450°C, (d) 1480°C, and (e) 1550°C for 6 h.

1 : 2 ordering superlattice reflections indicated by asterisk were found in all diffraction patterns. Therefore, the 1 : 2 ordered hexagonal structure is developed in all the specimens. The peaks for the second phase were not observed.

Fig. 2(a)-(d) exhibit SEM images taken from both the thermally etched and the fracture surfaces of the BCN ceramics sintered at various temperatures for 6 h. The specimens sintered below 1400°C have a homogeneous microstructure and the average grain size was about 1.5 μm. For the specimen sintered at 1420°C, grain growth started but some grains are already grown up as shown in Fig. 2(b). For the specimens sintered at 1450°C, the average grain size was 10 μm. A large amount of the liquid phase indicated by the arrow was found in the specimens sintered above 1400°C [see Fig. 2(b) and 2(c)], the presence of the liquid phase is responsible for the grain growth. The composition of the liquid phase was investigated using Energy Dispersive Spectroscopy (EDS) on the specimen shown in Fig. 2(c) and the results are illustrated in Table 1. The concentration of Ba, Co, and Nb ions in the matrix are close to those of the nominal compositions. However, in the liquid phase, the concentrations of

Table 1. Chemical Compositions of the Matrix and the Liquid Phase of Ba(Co₁/₃Nb₂/₃)O₃ Ceramics Sintered at 1450°C for 6 h

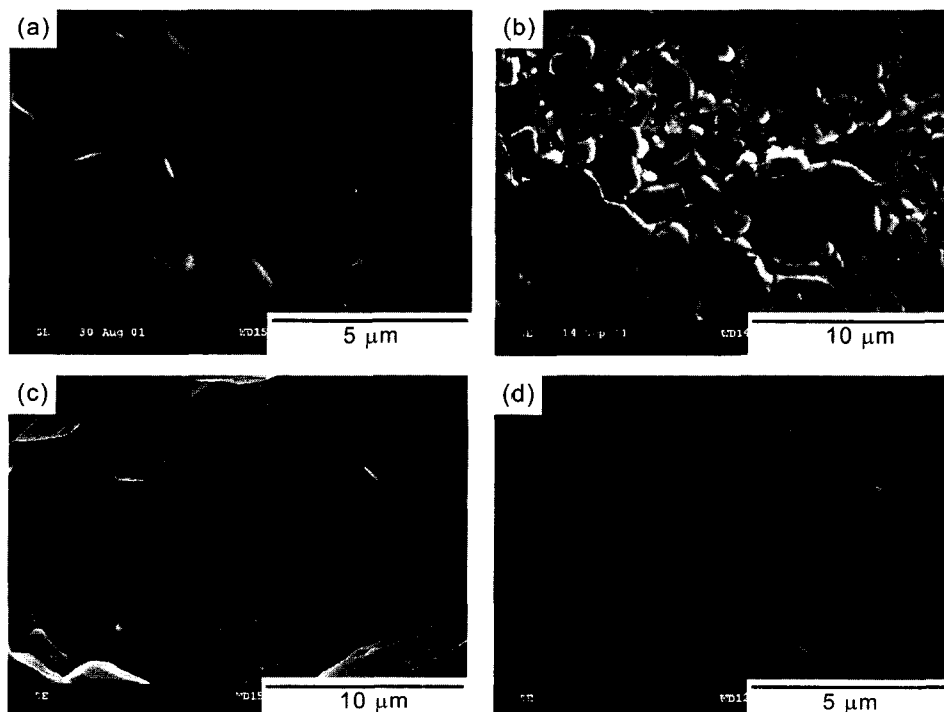| Element	Matrix (at%)	Liquid phase (at%)
Ba	53.12	43.36
Co	18.47	9.34
Nb	28.41	47.30

Fig. 2. SEM images of BCN ceramics sintered for 6 h at: (a) 1400°C, (b) 1420°C, (c) 1450°C (fracture surface), and (d) 1450°C (muffled with CoO).

Nb and Ba ions are high but that of Co ion is low. Therefore, the liquid phase is considered to be Ba- and Nb-rich phase.

Since the evaporation of the CoO was also observed for the BCN ceramics sintered at high temperature, the formation of the liquid phase in BCN ceramics could be related to the evaporation of CoO. In order to clarify the effect of the evaporation of CoO, BCN ceramics was sintered at 1450°C with CoO muffling to prevent the evaporation of CoO. Neither the liquid phase nor grain growth was observed in this specimen as shown in Fig. 2(d). Therefore, it can be suggested that the evaporation of CoO contributes to the formation of the liquid phase in BCN ceramics.

Variations of the relative density, dielectric constant, τ_f and Q×f value with sintering temperature are illustrated in
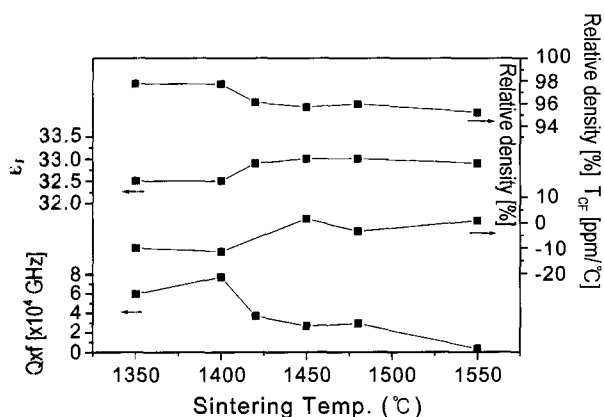

Fig. 3. Variations of the relative density, the dielectric constant, the temperature coefficient of the resonant frequency and Q×f value of BCN ceramics sintered at various temperatures for 6 h.

Fig. 3. The relative density of the specimens slightly decreased when the sintering temperature exceeded 1400°C but the decrease is not significant. The relative density of all the specimens was high above 95.5% of the theoretical density. The dielectric constant of the BCN sintered at 1350°C was about 32.7 and the variation of the dielectric constant with sintering temperature is not significant ranging between 32.5 and 33. The τ_f of the specimen sintered at 1350°C was about 10 ppm/°C and it increased when the sintering temperature exceeded 1400°C at which the microstructure of the specimen significantly changed. Therefore, the variation of the microstructure is considered to affect τ_f of the specimen but the details of the mechanism are not completely understood. Fig. 3 also shows the Q×f value of the specimens sintered at various temperatures. The Q×f value of the specimen sintered at 1350°C was about 60,000 GHz and it increased with sintering temperature showing the maximum value, 78,000 GHz, for the specimen sintered at 1400°C. However, it suddenly decreased when the sintering temperature exceeded 1400°C. The grain size increased with the sintering temperature and the relative density of all the specimens was high. Therefore, the deterioration of the Q-value cannot be explained by the variations of the grain size and the relative density. On the contrary, since a large amount of the liquid phase existed in the specimens sintered above 1400°C, the decrease of the Q-value could be due to the presence of the liquid phase.

3.2. Microstructure and Microwave Dielectric Properties of Ba(Zn$_{1/3}$Nb$_{2/3}$)O$_3$ Ceramics

Fig. 4(a)-(d) show the SEM images taken from the fracture surface of the BZN ceramics sintered at various tem-
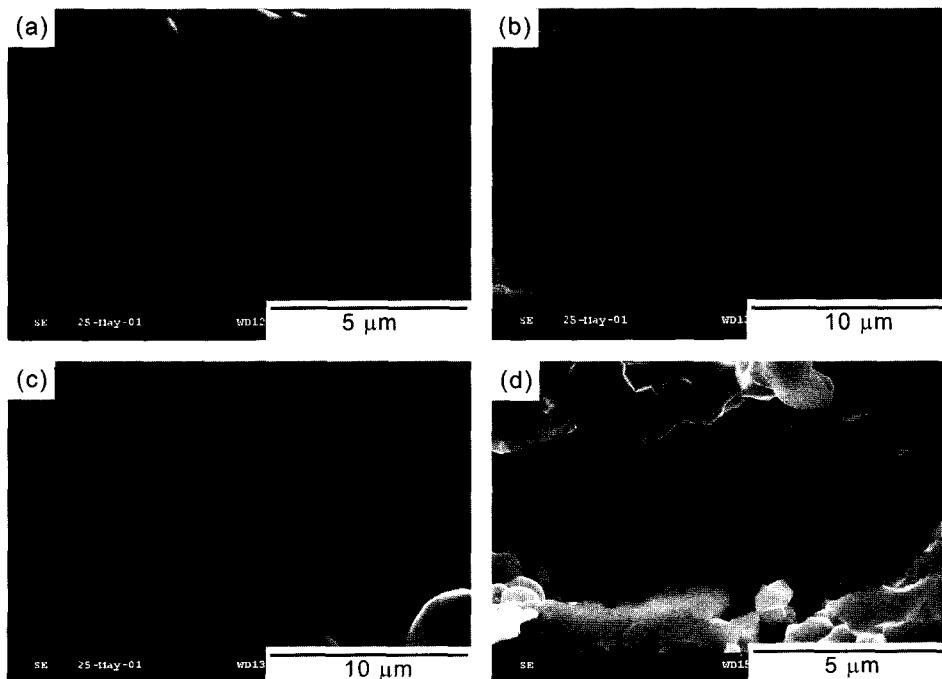

Fig. 4. SEM images of BZN ceramics sintered for 6 h at: (a) 1300°C, (b) 1350°C, (c) 1400°C, and (d) 1400°C muffled with ZnO.
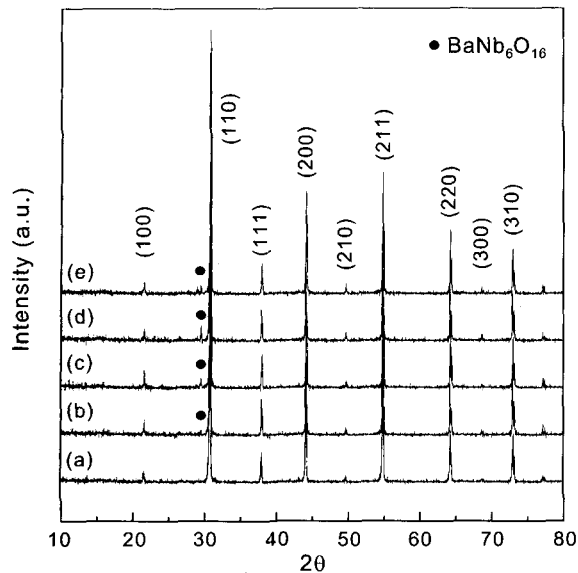
Fig. 5. X-ray diffraction patterns of BZN ceramics sintered for 6 h at: (a) 1300°C, (b) 1350°C, (c) 1400°C, (d) 1450°C, and (e) 1500°C.

peratures for 6 h. BZN sintered at 1300°C has a homogeneous microstructure and the average grain size was about 1.0 μm. When the specimen sintered at 1350°C, grain growth started and both small and large grains were found. For the specimen sintered at 1400°C, the homogeneous microstructure was developed with the average grain size of 10 μm. The liquid phase indicated by the arrow in Fig. 4(b) was observed in the specimens sintered above 1350°C and the presence of the liquid phase during sintering is responsible for the grain growth. It has been generally accepted that the liquid phase formed in BZN contains high concentrations of Ba and Nb ions. Therefore, it is considered that the liquid phase formed in our specimens must be Ba-

Nb phase. In order to find out the effect of the evaporation of ZnO on the formation of the liquid phase, BZN was sintered at 1400°C with ZnO muffling to prevent the evaporation of ZnO. The liquid phase and the grain growth were not observed in this specimen as shown in Fig. 4(d). Therefore, contrary to the previous results, which reported that the formation of liquid phase is due to the chemical inhomogeneity in the calcined powder, the evaporation of ZnO is responsible for the formation of the liquid phase in BZN ceramics.

Fig. 5 shows the X-ray diffraction patterns of BZN ceramics sintered at various temperatures. All the peaks were indexed in term of 1 : 2 ordered hexagonal unit cell. Peaks for 1 : 2 ordering were not observed in X-ray diffraction patterns but they were detected in electron diffraction pattern thus, BZN is considered to have a 1 : 2 ordered hexagonal structure. For the specimen sintered above 1350°C, $BaNb_6O_{16}$ second phase was found. However, for the specimens sintered at 1300°C, $BaNb_6O_{16}$ second phase was not observed. Therefore, the formation of $BaNb_6O_{16}$ second phase is attributed to the evaporation of ZnO. Since the liquid phase was found in the specimens sintered above 1350°C and the melting temperature of the $BaNb_6O_{16}$ phase is about 1320°C, it can be suggested that the liquid phase formed in our specimen has the composition similar to the $BaNb_6O_{16}$ phase.

Fig. 6(a)-(c) show the electron diffraction patterns obtained from the specimens sintered at various temperatures. The electron diffraction patterns show the 1 : 2 ordering superlattice reflections, which were not found in the X-ray diffraction patterns indicating that all the specimens have the 1 : 2 ordered hexagonal structure. For the specimen sintered at 1300°C, the intensity of the 1 : 2 ordering superlattice reflection is very strong but it suddenly decreased when the sintering temperature exceeded 1300°C. For the specimen sintered at 1500°C, new reflections
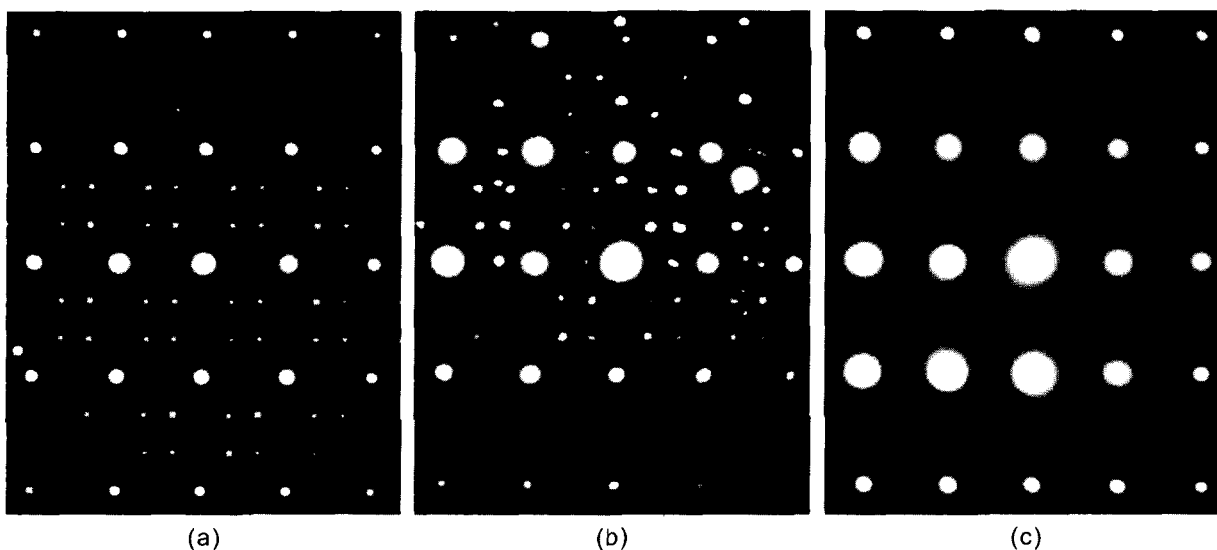

(a)   (b)   (c)

Fig. 6. Electron diffraction patterns of BZN ceramics sintered for 6 h at: (a) 1300°C, (b) 1350°C, and (c) 1500°C.
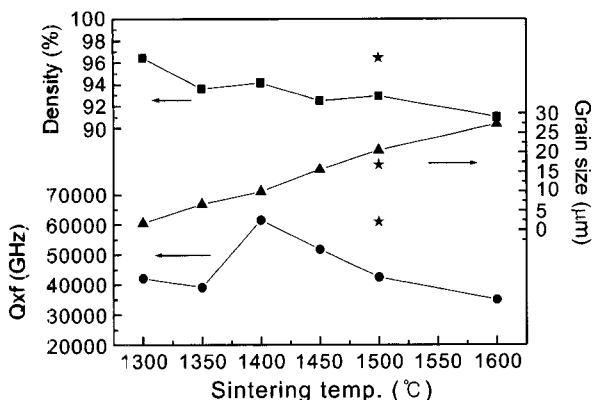
Fig. 7. Variations of the relative density, the average grain size and the Q×f value of BZN ceramics sintered at various temperatures for 6 h (★ : muffled BZN).

Fig. 8. X-ray diffraction patterns of the (1-x)BCN-xBZN ceramics with $0.0 \leq x \leq 1.0$ sintered at 1400°C for 6 h.

appeared at the 1/2(111) positions. These reflections are not the 1 : 1 ordering reflections but are the artifacts due to the overlap of the streaks in 1/3(111) positions.

Variations of the relative density, the grain size and the Q-value of BZN ceramics sintered at various temperatures for 6 h were illustrated in Fig. 7. The relative density of the specimen decreased with the increase of sintering temperature and it is due to the evaporation of ZnO. The relative density of BZN sintered at 1400°C was still high, 94.3% of the theoretical density but it was low for the specimens sintered above 1400°C. The average grain size of the specimen sintered at 1300°C was about 2 μm and increased with sintering temperature. For the specimen sintered at 1500°C, the average grain size was about 20 μm. The Q-value of BZN sintered at 1300°C was about 45,000 GHz and it slightly decreased when the specimen sintered at 1350°C. However, it increased when sintering temperature exceeded 1350°C and showed maximum value at 1400°C. Since the degree of the 1 : 2 ordering decreased with increasing sintering temperature, the improvement of Q-value with sintering temperature is not related to the 1 : 2 ordering. On the other hand, the average grain size, which increased with sintering temperature, might be responsible for the improvement of Q-value. For the specimens sintered above 1400°C, even though the grain size increased, the Q-value decreased and it could be due to the decrease of the relative density. In order to improve the relative density and to find out the effect of relative density on the Q-value, specimen muffled with the BZN powders was sintered at 1500°C for 6 h inside the closed Al_2O_3 crucible, which limited the evaporation of ZnO. As shown in Fig. 7, the average grain size is similar to that of the specimen sintered at normal condition. However, the relative density and the Q-value significantly improved. Therefore, the enhancement of the Q-value of BZN sintered inside the closed crucible is explained by the increase of the relative density. Moreover, it can be suggested that both the relative density and the grain size are important for the Q-value of BZN ceramics.
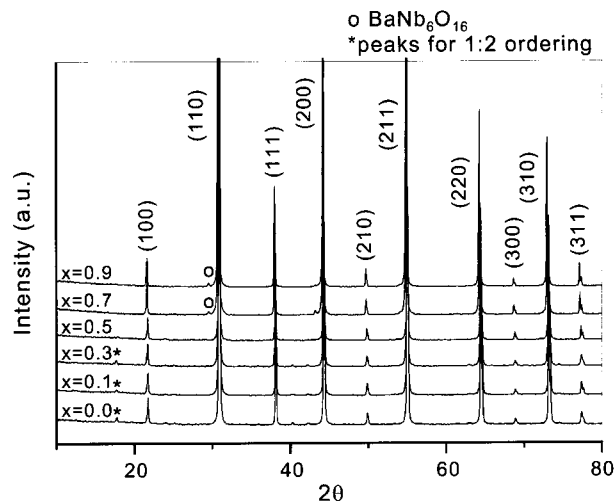
3.3. Microstructure and Microwave Dielectric Properties of $(1-x)Ba(Co_{1/3}Nb_{2/3})O_3$-$xBa(Zn_{1/3}Nb_{2/3})O_3$ Ceramics

Fig. 8 shows the X-ray diffraction patterns of the (1-x)$Ba(Co_{1/3}Nb_{2/3})O_3$-$xBa(Zn_{1/3}Nb_{2/3})O_3$ ceramics with $0.0 < x < 1.0$ sintered at 1400°C for 6 h. The 1 : 2 ordering shown in the specimens with $x \leq 0.3$ disappeared when x exceeded 0.3. According to the previous result, the 1 : 2 ordered structure which exists in BZN ceramics sintered at 1300°C, disappeared in the BZN ceramics sintered at 1400°C and it was explained by the evaporation of the ZnO.[3] Therefore, the disturbance of the 1 : 2 ordering occurred in the (1-x)$Ba(Co_{1/3}Nb_{2/3})O_3$-$xBa(Zn_{1/3}Nb_{2/3})O_3$ ceramics with $x > 0.3$ can be attributed to the evaporation of ZnO during sintering. The XRD patterns show that $BaNb_6O_{16}$ second phase, which was found in BZN also exists in the specimens with $x \geq 0.6$. In addition, X-ray analysis also carried out on the 0.7BCN-0.3BZN specimens sintered at various temperatures and the 1 : 2 ordering the disappeared for the specimens sintered above 1400°C. Thus, the transition temperature of the 1 : 2 ordering for the 0.7BCN-0.3BZN specimens is between 1400 and 1450°C.

Fig. 9(a)-(d) show the SEM images of the (1-x)$Ba(Co_{1/3}Nb_{2/3})O_3$-$xBa(Zn_{1/3}Nb_{2/3})O_3$ ceramics with $0.0 < x < 1.0$ sintered at 1400°C for 6 h. For the specimens with $x \leq 0.3$, the homogeneous microstructure without second phase was developed and the average grain size was about 2.5 μm. The grains of the specimen started to grow when x=0.5 and for the specimen with x=0.7, the grain growth was completed with the average grain size of 10 μm. The grain growth occurred for the BZN ceramics sintered above 1300°C and it is attributed to the presence of $BaNb_6O_{16}$ second phase whose melting temperature is about 1320°C.[3] Therefore, the grain growth occurred in the specimens with $x \geq 0.5$ also can be explained by the presence of $BaNb_6O_{16}$ second phase. From the XRD and SEM results, it can be suggested that the microstructure of the specimens with $x \leq 0.3$ is very similar to that of BCN ceramics and for specimens with $x \geq 0.5$, the micro-
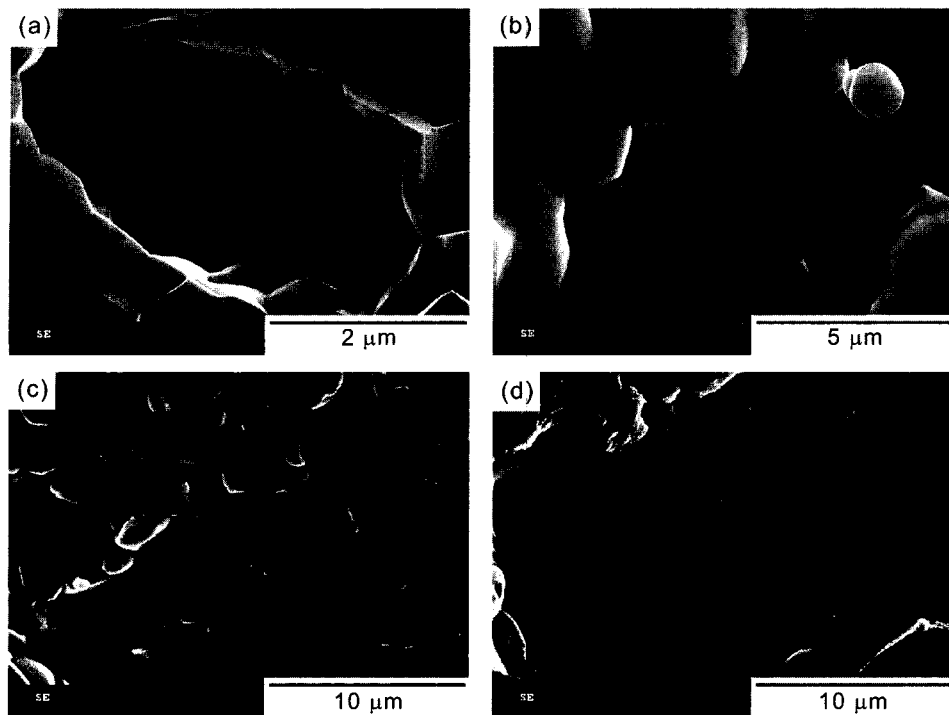
Fig. 9. SEM images of the (1-x)BCN-xBZN ceramics sintered at 1400°C for 6 h: (a) x=0.0, (b) x=0.3, (c) x=0.5, and (d) x=0.7.
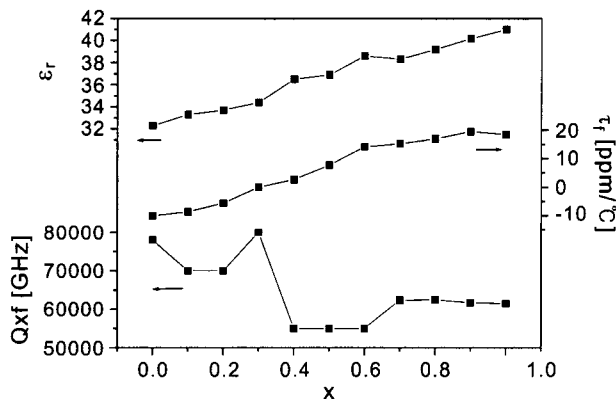

Fig. 10. Dielectric constant, temperature coefficient of the resonance frequency and Q×f value for the (1-x)BCN-xBZN ceramics with 0.0≤x≤1.0 sintered at 1400°C for 6 h.
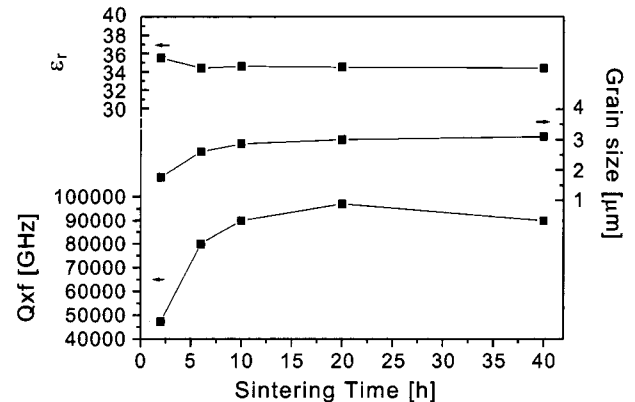

Fig. 11. Variations of the dielectric constant, the average grain size and the Q×f value of the 0.7BCN-0.3BZN ceramics sintered at 1400°C for various times.

structure is similar to that of BZN ceramics.

Variations of the τ_f, dielectric constant and Q×f value of the specimens were illustrated in Fig. 10. The τ_f linearly increased with the increasing x and it is close to zero when x=0.3. The dielectric constant of the BCN is about 33 and that of BZN is 41. The dielectric constant also linearly increased with the increase of x and it is about 34.5 for the 0.3BCN-0.7BZN ceramics, which has the zero τ_f. The Q-value of the specimens can be divided into two parts. For the specimens with x≤0.3, the Q×f value is high above 70,000 GHz, which is similar to that of BCN. On the contrary, for the specimens with x>0.3, it is similar to BZN about 55,000 GHz. Since the microstructure of the speci-

mens with x≤0.3 is similar to that of BCN ceramics and for the specimens with x≥0.5, the microstructure is similar to that of BZN ceramics, it is considered that the Q value of the (1-x)Ba(Co$_{1/3}$Nb$_{2/3}$)O$_3$-xBa(Zn$_{1/3}$Nb$_{2/3}$)O$_3$ ceramics is closely related to microstructure of the specimens.

According to the above results, the 0.7BCN-0.3BZN ceramics sintered at 1400°C has the excellent microwave dielectric properties of τ_f=0 ppm/°C, ε_r=34.5 and Q×f=80,000 GHz. Therefore, the detailed investigation was carried out on the 0.7BCN-0.3BZN ceramics. Fig. 11 illustrated the variations of the ε_r, average grain size and Q-value of the 0.7BCN-0.3BZN sintered at 1400°C for various times. The variation of the ε_r with sintering time is negligible ranged between 34 and 35. The grain size of the specimens sintered

for 2 h was about 1.7 µm and it increased with the increase of sintering time. Liquid phase or abnormal grain growth have not been observed in this system. The $Q \times f$ value of the specimen increased with the increase of sintering time and for the specimens sintered for 20 h, it was about 97,000 GHz. The variation of the Q-value with sintering time is similar to that of grain size therefore, the increase of the Q value with sintering time could be related to the increase of the grain size.

4. Conclusions

$Ba(Co_{1/3}Nb_{2/3})O_3$ ceramics has the 1 : 2 ordered hexagonal structure. The liquid phase containing high concentrations of Ba and Nb ions was observed for the specimens sintered above 1400°C. Grain growth occurred for the specimens sintered above 1400°C, which is due to the presence of the liquid phase during the sintering. The Q-value increased with increasing sintering temperature and the maximum Q-value was obtained for the BCN sintered at 1400°C.

BZN has the 1 : 2 ordered hexagonal structure and the degree of ordering has been decreased with the increase of sintering temperature. Liquid phase was observed for the specimens sintered above 1350°C. Grain growth occurred for the specimens sintered above 1350°C. The Q-value increased with increasing sintering temperature and the maximum Q-value was obtained for the specimen sintered at 1400°C for 6 h. The enhancement of the Q-value is not related to the 1 : 2 ordering but the increase of the grain size.

For the (1-x)BCN-xBZN ceramics, the 1 : 2 ordered hexagonal structure was observed in the specimens with $x \le 0.3$ and the $BaNb_6O_{16}$ second phase was found in the specimens with $x \ge 0.6$. The grain growth, which is related to the $BaNb_6O_{16}$ phase occurred in the specimens with $x \ge 0.5$. The τ_f increased with x and the specimens with $0.3 \le x \le 0.4$ have zero τ_f. The Q-value was high for the specimens with $x \pounds 0.3$ but it decreased when x exceeded 0.3. In this work, the excellent microwave dielectric properties of $\tau_f=0.0$ ppm/°C, $\varepsilon_r=34.5$ and $Q \times f=97,000$ GHz were obtained for the 0.7BCN-0.3BZN ceramics sintered at 1400°C for 20 h.

REFERENCES

1. M. Onoda, J. Kuwata, K. Kaneta, K. Toyama, and S. Nomura, "$Ba(Zn_{1/3}Nb_{2/3})O_3-Sr(Zn_{1/3}Nb_{2/3})O_3$ Solid Solution Ceramics with Temperature-stable High Dielectric Constant and Low Microwave Loss," *Jpn. J. Appl. Phys.*, **21** 1707-10 (1982).

2. K. S. Hong, I. T. Kim, and C. D. Kim, "Order-disorder Phase Formation in the Complex Perovskite Compounds $Ba(Ni_{1/3}Nb_{2/3})O_3$ and $Ba(Zn_{1/3}Nb_{2/3})O_3$," *J. Am. Ceram. Soc.*, **79** 3218-24 (1996).

3. S. Y. Noh, M. J. You, S. Nahm, C. H. Choi, H. M. Park, and H. J. Lee, "Effect of Structural Changes on the Microwave Dielectric Properties of $Ba(Zn_{1/3}Nb_{2/3})O_3$ Ceramics," *Jpn. J. Appl. Phys.*, **41** 2978-81 (2002).

4. I. T. Kim, K. S. Hong, and S. J. Yoon, "Effects on Non-stoichiometry and Chemical Inhomogeneity on the Order-disOrder Phase Formation in the Complex Perovskite Compounds, $Ba(Ni_{1/3}Nb_{2/3})O_3$ and $Ba(Zn_{1/3}Nb_{2/3})O_3$," *J. Mat. Sci.*, **30** 514-21 (1995).

5. J. S. Sun, J. J. Yu, J. C. You, and C. C. Wei, "Microwave Dielectric Properties of $Ba(Sn_xZn_{(1-x)/3}Nb_{(1-x)2/3})O_3 (0 \le x \le 0.32)$ Ceramics," *J. Mat. Sci.*, **28** 2163-68 (1993).

6. C. C. You, C. L. Huang, C. C. Wei, and J. W. Huang, "Improved High-Q Dielectric Resonator Sintered at Low Firing Temperature," *Jpn. J. Appl. Phys.*, **34** 1911-15 (1995).

7. J. S. Kim, J. H. Lee, Y. S. Lim, J. W. Jang, and I. T. Kim, "Revisit to the Anomaly in Dielectric Properties of $(Ba_{1-x}Sr_x)(Zn_{1/3}Nb_{2/3})O_3$ Solid Solution System," *Jpn. J. Appl. Phys.*, **36** 5558-61 (1997).

8. K. Endo, K. Fujimoto, and K. Murakawa, "Dielectric Properties of Ceramics in $Ba(Co_{1/3}Nb_{2/3})O_3-xBa(Zn_{1/3}Nb_{2/3})O_3$ Solid Solutions," *J. Am. Ceram. Soc.*, **70** C-215-C-18 (1987).

9. B. W. Hakki and P. D. Coleman, "Dielectric Resonator Method of Measuring Inductive Capacities in the Millimeter Range," *IRE. Trans. Microwave Theory Tech.*, **8** 402-10 (1960).

10. W. E. Courtney, "Analysis and Evaluation of a Method of Measuring the Complex Permittivity of Microwave Insulators," *IEEE Trans. Microwave Theory Tech.*, **MTT-18** 476-85 (1970).